A Simplified Stability Analysis for Modern A.C. Feeder Voltage Control Using Multiple Power Converters for Shinkansen Systems

K. Kunomura* and T. Koseki**

* Central Japan Railway Company, 2-1-85 Konan, Minato-Ku, Tokyo, Japan

** The University of Tokyo, 7-3-1 Hongo, Bunkyo-Ku, Tokyo, Japan

***Abstract*--Recent faster and more frequent train service at Tokaido Shinkansen makes it difficult to stabilize the feeding voltage only by compensating reactive power. Therefore, the active power compensation between two phases has been introduced for further stabilization of the voltage, and the converter control strategy called "fixed power-factor method" was applied in the commercial operation that started in February 2009. The active power compensation to control a feeder voltage stably is substantially more complicated than the conventional reactive power compensation. This paper describes a novel stability judging method, based on a model including multiple power converters, significant for indicating appropriate active/reactive compensation strategies to the operator of the new Shinkansen power supply system.**

***Index Terms*—A.C. voltage control, Linearized circuit model, Power converters, Tokaido Shinkansen**

I. Introduction

Recent frequenter train service and higher accelerating performance of rolling stocks request more real power to the electrification system at Tokaido Shinkansen, the high speed ground transportation in Central Japan. This large demand of the active power causes considerable voltage fluctuation. Conventional reactive power compensation is being not sufficient for stable electric power supply in electrified sections where line impedance is relatively large. Power converters which can supply active power for stabilizing voltage with specified constant power factor are being introduced to the commercial line for solving the problem recently [1].

The sensitivity of such converters from their power compensation to the voltage change is large. That is to say, the active power compensation for the voltage stabilization is substantially more difficult than the conventional reactive power compensation. A systematic tuning of controllers of power converters is requested for stabilizing voltage control for electrification circuit with large line impedance.

EMTP, Electro Magnetic Transient Program, is a popular tool to numerically calculate transient response of AC-electrification system, and good agreements with real measurement are well-known [2]. However, the numerical calculations for complicated electrification circuits are time-consuming, and the numerical simulations for evaluating performances of different controllers with various combinations of design parameters are often too heavy for practical applications. Also visual representation of the stability is useful for efficient design of voltage stabilizing controllers, but the numerical calculation such as EMTP does not give such straightforward visibility [3]. This paper is presenting a methodology for efficient and straightforward design of the voltage controller by introducing simplified equivalent linear model of electrification circuit including multiple power converters.

II. Simplified Linear Model Equivalent to Electrification System

A. Block Diagram of a Electrification System Including Multiple Power Converters

As the first step for introducing linearized equivalent model of an electrification system including multiple power converters, we have derived a block diagram representing the transfer characteristic from voltage disturbance at a connecting point of a power converter to line as an input to change of voltage of the same connecting point as an output.

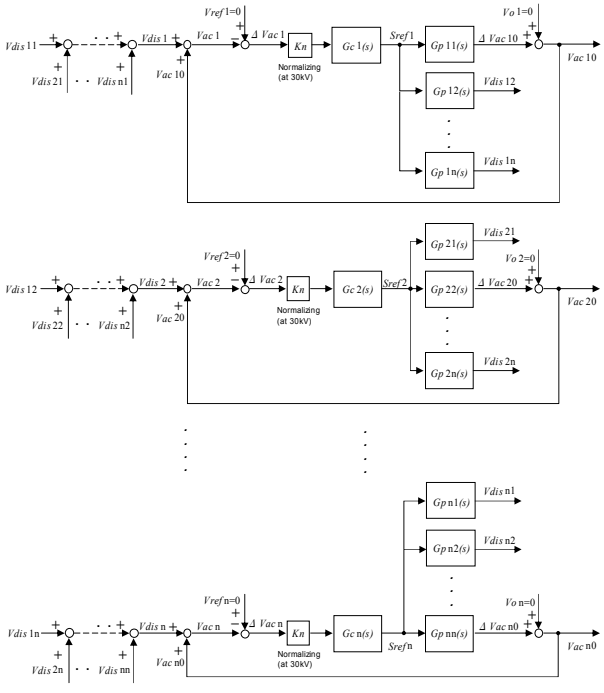

Fig. 1. Block diagram of feeding system using n- power converters.

An example of electrification system including two power converters will be discussed in detail in this

chapter for simplicity. This modeling method can be extended to handle generic electrification system including arbitrary number of converters in principle.

Fig. 1 shows a block diagram representing electrification system which has power converters for regulating voltage at n-points. *Vdis*nn is a disturbance voltage at the n-th connecting point. *Gc*n is the transfer function of the voltage regulator at the n-th converter.

*Gp*1n is the transfer function from the output voltage of the converter No. 1 as a system input to the voltage change at the n-th connecting point caused by the power converter No. 1 as a system output. The transfer functions to the output of the n-th power converters are defined as *Gp*n1, ... *Gp*nn in the same way.

B. Polynomial Approximation of Voltage Response Waveform of an Electrification

Gp, the transfer function from the converter output power to the voltage change at connecting point of the converter is unknown in Fig. 1. This transfer characteristic is approximately identified by observing the voltage-change waveform when a step input is supplied to a real plant experimentally, or plant model in a numerical simulator using EMTP. The transfer function is well approximated by a second order delay empirically.

The stability and performance of the voltage control is especially significant when the electric loads are heavy. The experimental identification to measure the input response at a real plant is, of course, difficult when the electric loads by running trains are heavy. Just the identification using EMTP-simulator is, therefore, used for such heavy load cases.

The following data show the specification of the feeding circuit and train load conditions for a case study of the step input test for transfer characteristic identification using EMTP-numerical circuit calculation. A standard circuit with two power converters is studied for this case study.

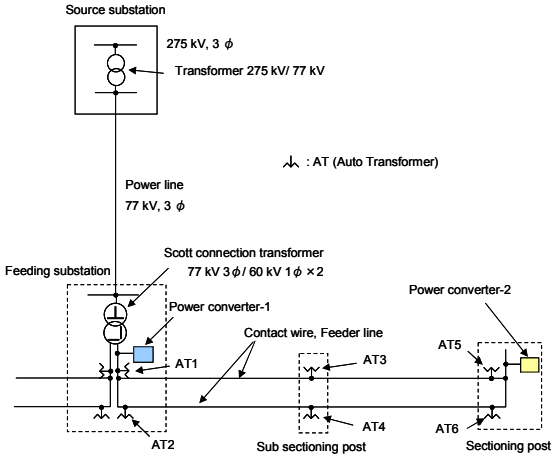

Fig. 2. Power diagram of an electric feeding system.

Fig. 2 shows an electric feeding system for a case study. The power converter 1 is a self-commutated converter, and it can supply commanded power to the system regardless of the voltage at the connection point, if the request of the output current is under its rated current. On the other hand, the converter 2 is a thyristor-controlled transformer as a static var compensator, whose operation depends on the external voltage conditions. The rated capacities of the converter 1 and 2 are 50 MVA and 35 MVA, respectively.

Fig. 3 shows train load conditions for the case study. The numbers in the figure indicate the distances from a feeding substation. The current value in the figure means the condition when the voltage at the pantograph is 25 kV. The train is a power-constant electric load whose power factor is always controlled to unity. The starting time profile of the train load is assumed in the simulation as follows: No.1: 0.2 sec→0.35 sec, No.2: 0.4 sec→0.55 sec, No.3: 0.6 sec→0.75 sec, No.4: 0.8 sec→0.95 sec, No.5: 1.0 sec→1.15 sec, and No.6: 9.0 sec→10.0 sec.

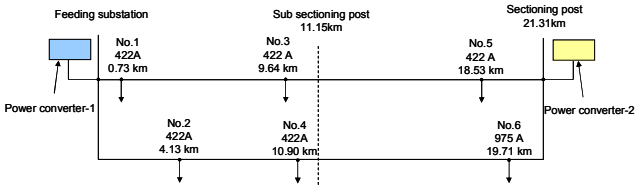

Fig. 3. Position of train load.

The voltage changes at the connecting points 1 and 2 are calculated by giving stepwise power changes of the converter for identifying the transfer function *Gp*.

The gradient of the PV-curve is larger when real power of load is large, in general. The response of the voltage depends on the range of the feeding voltage amplitude. The change of the voltage is more sensitive, when the voltage is lower, i.e., the load is larger. For studying serious cases in realistic operation, the voltage response was calculated in the range between 26.0 kV and 26.5 kV in this case study. The sensitivity of the voltage change is small in high feeding voltage range, hence the higher stability of the operation of voltage compensator is expected. Therefore the controller design of the voltage stabilizer in low voltage range is conservative.

Fist of all, the output reactive powers of the converters 1 and 2 were calculated so that the voltages at the connecting points of the two converters could be 26.0 kV under the full train load in Fig. 3. The EMTP numerical simulator calculated the output reactive powers as 0.387 p.u. and 0.480 p.u. of converters 1 and 2, respectively, for the 26.0 kV at the connecting point.

Next, the reactive powers which make connecting point voltages 26.5 kV were calculated from the EMTP-simulator. The resultant output reactive powers of the converters 1 and 2 were 0.407 p.u. and 0.508 p.u., respectively. These mean 0.020 p.u. and 0.028 p.u., respectively, additional to the initial case.

The initial condition was, therefore, set that the output of the converter 1 was 0.387 p.u. and the output of the converter 2 was 0.480 p.u. and the step inputs of 0.020 p.u. and 0.028 p.u. were applied to the two converters, respectively. Then the voltage changes at the connecting points were calculated by the EMTP-simulator.

The calculated step response is shown in Fig. 4. The step input was applied at 15 sec. in the case study.

The transfer function is approximated to a second-

order delay. Gain Kv, damping factor ζ and natural angular frequency ω_n of the approximate second-order system are determined from the overshoot, the amplitude of the voltage change and the settling time. The parameters of the case in Fig. 4 is determined as Kv=27200, the damping factor ζ =0.99, and the natural angular frequency ω_n =15 rad/s. The transfer function $Gp11$ is therefore written in equation (1). The step response of the approximate transfer function is shown by the dotted line in Fig. 4.

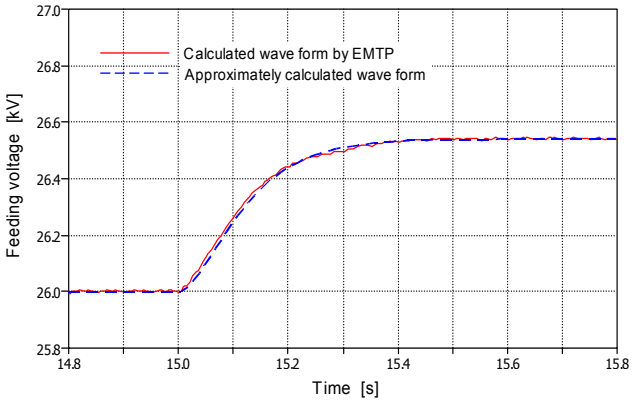

Fig. 4. Step response of the feeding voltage.

$$Gp11 = \frac{27200 \cdot 15^2}{s^2 + 2 \cdot 0.99 \cdot 15s + 15^2} \tag{1}$$

The transfer function $Gp12$ was identified by applying step input of 0.020 p.u. to the converter 1 and calculating the voltage of the connecting point to the converter 2, and $Gp22$ was identified by applying step input of 0.028 p.u. to the converter 1 and calculating the voltage of the connecting point to the converter 2, in the same way.

C. Linear Circuit Model for the Response of Feeding Voltage

At first, we will drive a linear circuit model for the response of feeding voltage to the output of converters modeled as a second order delay.

$Gp(s)$ the transfer function of the response of the feeding voltage is written in (2). The output $Y(s)$ means the response of the feeding voltage, the $U(s)$ means the output power of the converters.

$$Gp(s) = \frac{Y(s)}{U(s)} = \frac{Kv \cdot \omega_n^2}{s^2 + 2\zeta\omega_n \cdot s + \omega_n^2} \tag{2}$$

The following equation (3) is derived from (2).

$$\frac{Y(s)}{X(s)} \cdot \frac{X(s)}{U(s)} = Kv \cdot \frac{\omega_n^2}{s^2 + 2\zeta\omega_n \cdot s + \omega_n^2} \tag{3}$$

The following equation is derived from (3).

$$\left(s^2 + 2\zeta\omega_n \cdot s + \omega_n^2\right) X(s) = \omega_n^2 \cdot U(s)$$

$$\ddot{x}(t) + 2\zeta\omega_n \cdot \dot{x}(t) + \omega_n^2 \cdot x(t) = \omega_n^2 \cdot u(t)$$

The state equation (4) is derived from $x(t) = x_1$, and $\dot{x}(t) = x_2$.

$$\dot{x}_2 = -\omega_n^2 \cdot x_1 - 2\zeta\omega_n \cdot x_2 + \omega_n^2 \cdot u(t) \tag{4}$$

The output equation (5) is derived from (3) in the same way.

$$Y(s) = Kv \cdot X(s)$$

$$y(t) = Kv \cdot x_1 \tag{5}$$

Fig. 5 shows the approximate linear circuit model of the feeding voltage response based on the state equation representation.

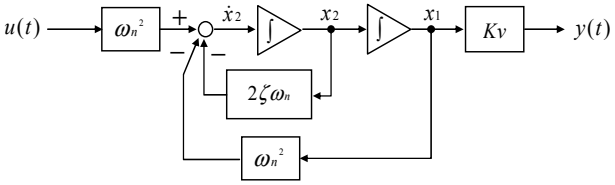

Fig. 5. The linearized circuit model of the feeding voltage response.

D. Linear Circuit Model of AC-Voltage Regulator

The transfer characteristic of the AC-voltage regulator can be directly derived from its control rule. For instance, when the controllers of the converter 1 and the converter 2 are designed as proportional + first-order delay and first-order delay, respectively, the transfer functions of the converter 1 and the converter 2 are described as (6) and (7), respectively. Kp_1, K_1, and T_1 mean the gain of the proportional controller, the gain and the time constant of the first-order delay controller of the converter 1, respectively. K_2 and T_2 mean the gain and the time constant of the first-order delay controller of the converter 2, respectively, in the same way.

$$Gc1 = Kp_1 + \frac{K_1}{1 + T_1 s} \tag{6}$$

$$Gc2 = \frac{K_2}{1 + T_2 s} \tag{7}$$

The linear model of the first-order delay is derived as follows. The equation is derived, when the input and the output of the controller are $U(s)$ and $Y(s)$ respectively.

$$\frac{Y(s)}{U(s)} = \frac{K}{1 + Ts}$$

The following equations are derived from the above equation as follows.

$$\frac{Y(s)}{X(s)} \cdot \frac{X(s)}{U(s)} = K \cdot \frac{1}{1 + Ts} \tag{8}$$

$$(1 + Ts) X(s) = U(s)$$

$$T \cdot \dot{x}(t) + x(t) = u(t)$$

The state equation (9) is derived from (8), $x(t) = x_1$, and $\dot{x}(t) = x_2$.

$$x_2 = -\frac{1}{T} x_1 + \frac{1}{T} u(t) \tag{9}$$

The output equation (10) is derived from (8) in the same way.

$$Y(s) = K \cdot X(s)$$

$$y(t) = K \cdot x_1 \tag{10}$$

Fig. 6 summarizes the transfer characteristic of the first-order delay based on the linear state-space representation in (9) and (10). Since the controller of proportional + first-order delay is superposition of the two controllers, it is graphically summarized as Fig. 7.

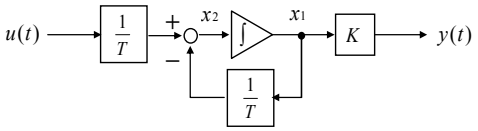

Fig. 6. The linearized circuit model of the first order control.

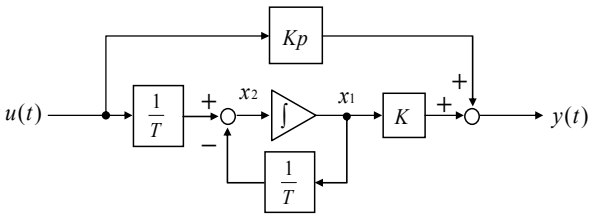

Fig. 7. The linearized circuit model of the proportional control and the first order control.

E. Linear Model of the Total Feeding System

Fig. 8 shows the linear model of the total feeding system by combining subsystems figures 1, 5, 6, and 7.

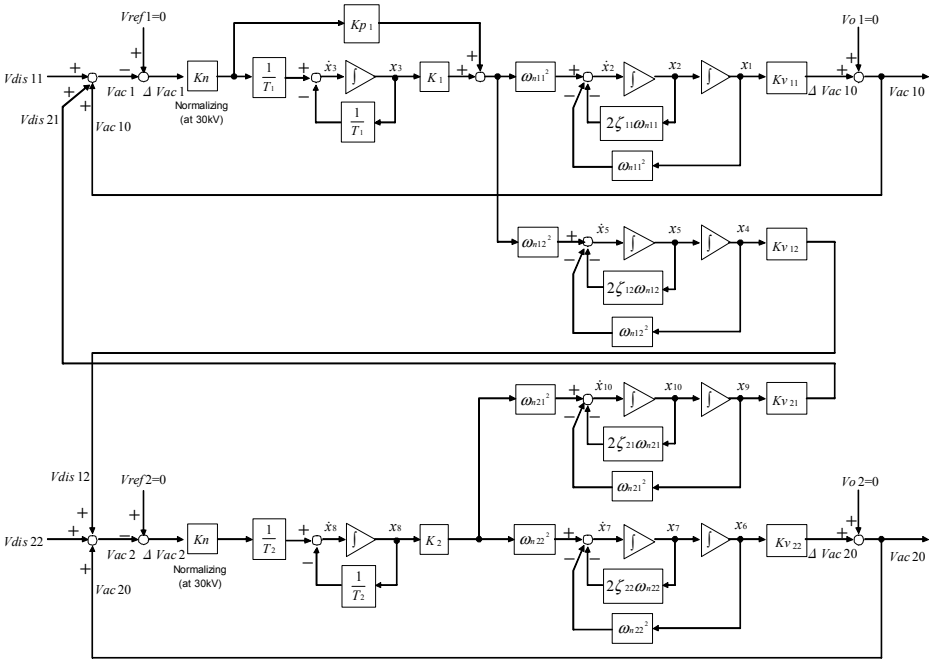

Fig. 8. The linearized circuit model of the feeding system using two power converters.

III. Derivation of State Space Representation and Calculation of Pole Locations

A. Simultaneous equations for the state variables

The simultaneous ten first-order differential equations are derived from the linear model in Fig. 8 as follows.

$$\dot{x}_1 = x_2$$

$$\dot{x}_2 = -\omega_{n11}^2 \cdot x_1 - 2\zeta_{11}\omega_{n11} \cdot x_2 + \omega_{n11}^2 K_1 \cdot x_3 - \omega_{n11}^2 Kp_1 Kn \cdot (Kv_{11} \cdot x_1 + Kv_{21} \cdot x_9 + Vdis11)$$

$$\dot{x}_3 = -\frac{1}{T_1} \cdot x_3 - \frac{Kn}{T_1} \cdot (Kv_{11} \cdot x_1 + Kv_{21} \cdot x_9 + Vdis11)$$

$$\dot{x}_4 = x_5$$

$$\dot{x}_5 = \omega_{n12}^2 K_1 \cdot x_3 - \omega_{n12}^2 \cdot x_4 - 2\zeta_{12}\omega_{n12} \cdot x_5 - \omega_{n12}^2 Kp_1 Kn \cdot (Kv_{11} \cdot x_1 + Kv_{21} \cdot x_9 + Vdis11)$$

$$\dot{x}_6 = x_7$$

$$\dot{x}_7 = -\omega_{n22}^2 \cdot x_6 - 2\zeta_{22}\omega_{n22} \cdot x_7 + \omega_{n22}^2 K_2 \cdot x_8$$

$$\dot{x}_8 = -\frac{1}{T_2} \cdot x_8 - \frac{Kn}{T_2} \cdot (Kv_{22} \cdot x_6 + Kv_{12} \cdot x_4 + Vdis22)$$

$$\dot{x}_9 = x_{10}$$

$$\dot{x}_{10} = \omega_{n21}^2 K_2 \cdot x_8 - \omega_{n21}^2 \cdot x_9 - 2\zeta_{21}\omega_{n21} \cdot x_{10} \qquad (11) \text{ to } (20)$$

B. Synthesis of Total State Equation

The total state equation shall be derived in this section. The state equation of the feeding system is defined in (21).

$$\dot{\mathbf{x}} = \mathbf{A}\mathbf{x} + \mathbf{B}\mathbf{u} \qquad (21)$$

The input vector **u** of (21) is written as (22), since the disturbance-input to the feeding system is modeled as the voltage change caused by the change of train load in Fig. 1.

$$\mathbf{u} = \begin{bmatrix} Vdis11 \\ Vdis22 \end{bmatrix} \qquad (22)$$

Hence, the input matrix **B** (10X2) in (21) is written in (23), from the simultaneous equations (11) to (20).

$$\mathbf{B} = \begin{bmatrix} 0 & 0 \\ -\omega_{n11}^2 Kp_1 Kn & 0 \\ -\frac{Kn}{T_1} & 0 \\ 0 & 0 \\ -\omega_{n12}^2 Kp_1 Kn & 0 \\ 0 & 0 \\ 0 & 0 \\ 0 & -\frac{Kn}{T_2} \\ 0 & 0 \\ 0 & 0 \end{bmatrix} \qquad (23)$$

$$\mathbf{A}=\begin{bmatrix}
0 & 1 & 0 & 0 & 0 & 0 & 0 & 0 & 0 & 0 \\
-\omega_{n11}^2(1+Kp_1KnKv_{11}) & -2\zeta_{11}\omega_{n11} & \omega_{n11}^2K_1 & 0 & 0 & 0 & 0 & 0 & -\omega_{n11}^2Kp_1KnKv_{21} & 0 \\
-\frac{KnKv_{11}}{T_1} & 0 & -\frac{1}{T_1} & 0 & 0 & 0 & 0 & 0 & -\frac{KnKv_{21}}{T_1} & 0 \\
0 & 0 & 0 & 0 & 1 & 0 & 0 & 0 & 0 & 0 \\
-\omega_{n12}^2Kp_1KnKv_{11} & 0 & \omega_{n12}^2K_1 & -\omega_{n12}^2 & -2\zeta_{12}\omega_{n12} & 0 & 0 & 0 & -\omega_{n12}^2Kp_1KnKv_{21} & 0 \\
0 & 0 & 0 & 0 & 0 & 0 & 1 & 0 & 0 & 0 \\
0 & 0 & 0 & 0 & 0 & -\omega_{n22}^2 & -2\zeta_{22}\omega_{n22} & \omega_{n22}^2K_2 & 0 & 0 \\
0 & 0 & 0 & -\frac{KnKv_{12}}{T_2} & 0 & -\frac{KnKv_{22}}{T_2} & 0 & -\frac{1}{T_2} & 0 & 0 \\
0 & 0 & 0 & 0 & 0 & 0 & 0 & 0 & 0 & 1 \\
0 & 0 & 0 & 0 & 0 & 0 & 0 & \omega_{n21}^2K_2 & -\omega_{n21}^2 & -2\zeta_{21}\omega_{n21}
\end{bmatrix} \tag{24}$$

The system matrix **A** (10X10) in (21) is written in (24) , from the simultaneous equations (11) to (20).

The state equation in (21) has been derived in this way from (22), (23) and (24).

Next, the output equation (25) is derived as follows.

$$\mathbf{y}=\mathbf{Cx}+\mathbf{Du} \tag{25}$$

The output vector **y** of the feeding system in (25) is derived from Fig. 1 and written in (26).

$$\mathbf{y}=\begin{bmatrix} Vac1 \\ Vac2 \end{bmatrix} \tag{26}$$

The following relationship among $Vac1$, $Vac2$ and each state variable is derived from Fig. 8.

$$Vac1=Kv_{11}\cdot x_1+Kv_{21}\cdot x_9+Vdis11 \tag{27}$$

$$Vac2=Kv_{22}\cdot x_6+Kv_{12}\cdot x_4+Vdis22 \tag{28}$$

The output matrices **C** and **D** are calculated as follows, since the input vector **u** is written in (22).

$$\mathbf{C}=\begin{bmatrix} Kv_{11} & 0 & 0 & 0 & 0 & 0 & 0 & 0 & Kv_{21} & 0 \\ 0 & 0 & 0 & Kv_{12} & 0 & Kv_{22} & 0 & 0 & 0 & 0 \end{bmatrix} \tag{29}$$

$$\mathbf{D}=\begin{bmatrix} 1 & 0 \\ 0 & 1 \end{bmatrix} \tag{30}$$

C. Pole Location of the Total System

The system pole can be directly calculated from the linear state equation in (21). The system poles are the given-values of the system matrix **A**.

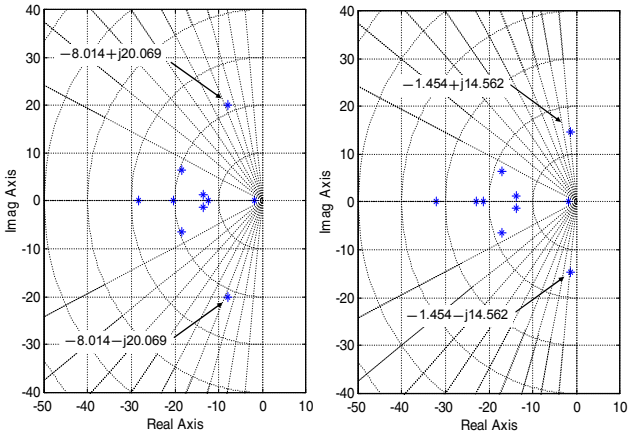

(a) Kp_1=2 (b) Kp_1=0

Fig. 9. The calculation result of the pole location of the feeding system.

System poles are plotted in Fig. 9 by giving typical controller parameters of converters 1 and 2 in Fig. 2.

Fig. 9 (a) is the case when Kp_1=2, K_1=20 and T_1=1 for the "proportional + first-order delay" controller of the converter 1 and K_2=10 and T_2=1 for the first-order delay controller of the converter 2.

Fig. 9 (b) is the case when Kp_1=0 for the controller of the converter 1, where other parameters are set identical to the case of Fig 9 (a).

The cosine of the angle between negative real axis and a line connecting original point and a pole means damping factor, which represents margin of the stability of the linear system intuitively. The comparison of Figs. 9 (a) and (b) shows that the proportional gain in the controller of the converter 1 plays a significant role to the stabilization of the voltage regulation.

This approach gives designers of the controllers efficient calculation of the dynamic performance and straightforward view on the system stability in the controller tuning.

IV. Verification in Comparison with Nonlinear Numerical EMTP-Calculation

We have compared the calculated results by the linear circuit model of the feeding system and the approximated linear second order delay subsystem with the calculated results by EMTP which can handle the circuit-non-linearity directly for verifying the proposed simplified approach.

The conditions of the power diagram and train loads were set similarly to Fig. 2 and Fig. 3 respectively. The voltage commands between trolley wire and feeder line to the voltage regulators of the power converters 1 and 2 were set as 53 kV and 51 kV respectively, for calculating the voltage at the connecting point of power converters in a same range. These values correspond to twice of 26.5 kV and 25.5 kV between trolley wire and rail.

The results calculated by EMTP are shown in Figs. 10 (a) and (b). These figures are the cases where the controller parameters are set identical to the cases of Figs. 9 (a) and (b) respectively.

As shown in Fig. 10 (a), even after all train loads start, the feeder voltage is controlled stably in this case. Therefore, the calculated result of the pole location in Fig. 9 (a) is appropriate.

On the other hand, the feeder voltage is oscillating largely after all train loads start in the case in Fig. 10 (b). Hence, the calculated result of the pole location in Fig. 9 (b) indicating less damping is correct.

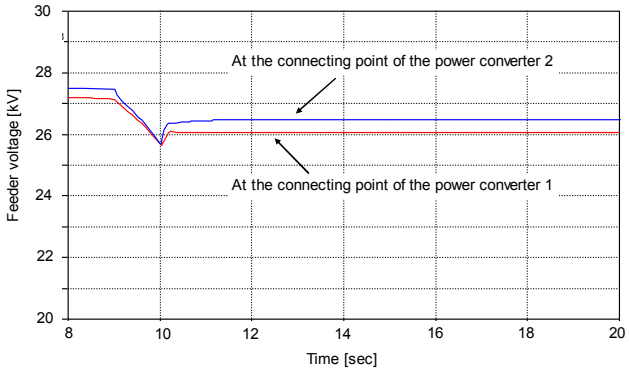

(a) Kp_1=2

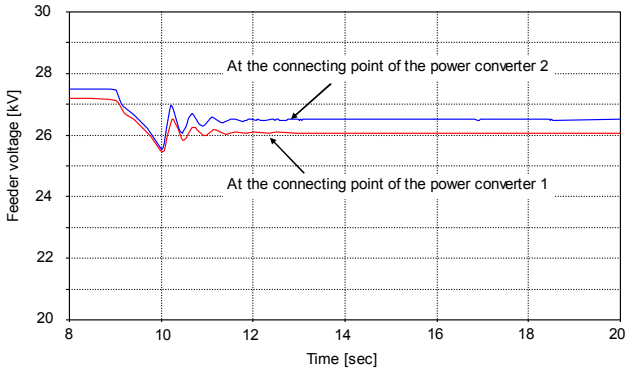

(b) Kp_1=0

Fig. 10. The calculation results by EMTP.

V. Experimental Verification at Commercial Shinkansen Line

The proposed design method for voltage regulator controllers has been applied to fixed power-factor converters as an electronic frequency changer (EFC) at Numazu frequency conversion substation of Tokaido Shinkansen commercial line. The voltage affected by real train operation has been measured for the verification of the proposed voltage regulator design.

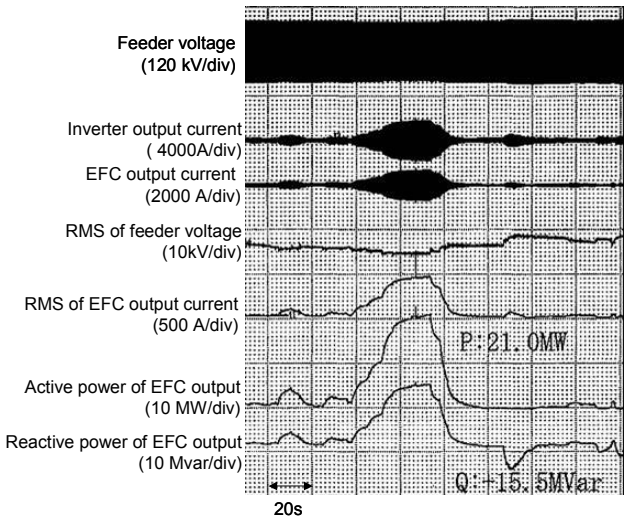

Fig. 11. The measuring data with real train load.

A result is shown in Fig. 11. The output of the EFC effectively stabilizes the voltage fluctuation between 54.9 kV and 59.0 kV of the feeding system of nominal substation voltage of 60.0 kV. It means that the regulator operation fulfills the required specification. This application proves the usefulness of the proposed design method in practice.

VI. Conclusions

We have derived a simplified straightforward method of stability analysis for an AC-electrification system including multiple power converters which control the feeder voltage. Results of the new simplified analysis have been compared with conventional EMTP-calculation which can handle the circuit-non-linearity directly, and they have shown good agreements.

(a) The transfer function from the output power of a converter to the voltage change of the converter connecting point has been approximated as linear second order delay. The plant parameter has been identified by a step response test of the EMTP-numerical model.

(b) The simplified linear circuit model of the feeding system is represented by a block diagram and the transfer function.

(c) An approximated linear state- and output- equations of total feeding system have been derived by combining the simplified linear models of subsystems. The pole location of the synthesized linear system has been calculated for checking the stability and performance of the control of feeding voltage regulators in a straightforward way.

The proposed simplified method gives a much more efficient feeding voltage analysis and systematic controller design than conventional cut-and-try method using many results of EMTP-numerical calculations.

Furthermore, it is advantageous for controller designer, to whom the pole locations visually show the stability margin of the voltage control, and this information enables a straightforward and systematic way of controller tuning.

The usefulness and dependability of the stability analysis using simplified linear model has been verified by the real application to the controller design of electronic frequency converter at Numazu frequency conversion substation of Tokaido Shinkansen. The frequency converter designed by the proposed method continues its successful operation presently.

References

[1] K. Kunomura, M. Onishi, M. Kai, N. Iio, M. Otsuki and T. Ishizuka, “Electronic Frequency Converter Controls A.C. Voltage Using Fixed Power Factor Method”, *IEEJ Trans. IA*, Vol.129, No.7, pp.768－774 (2009-7) (in Japanese)

[2] K. Ito, N. Nagayama, M. Otsuki, T. Ishizuka, F. Aoyama, T. Yoshino, J. Takazane, M. Oki and K. Kunomura, “Electronic Frequency Converter”, Proc. of the 2004 JIAS Conf., III, pp.347－352(2004)(in Japanese)

[3] Y. Shinki, A. Koyama, K. Temma and N. Morishima, “Study of SVG control under the change of power system configuration”, IEEJ PE-08-172 (2008-12) (in Japanese)